

See discussions, stats, and author profiles for this publication at: <https://www.researchgate.net/publication/258770057>

Integrated 1D/2D/3D Simulation of Fuel Injection and Nozzle Cavitation

Article in SAE International Journal of Engines · September 2013

DOI: 10.4271/2013-24-0006

CITATIONS

6

READS

3,128

3 authors:



Valdas Caika

AVL LIST GMBH

11 PUBLICATIONS 99 CITATIONS

[SEE PROFILE](#)



Peter Sampl

AVL LIST GMBH

21 PUBLICATIONS 289 CITATIONS

[SEE PROFILE](#)



David Greif

AVL LIST GMBH

56 PUBLICATIONS 284 CITATIONS

[SEE PROFILE](#)

Some of the authors of this publication are also working on these related projects:



Immersion quenching [View project](#)



Internal nozzle flow [View project](#)

Integrated 1D/2D/3D Simulation of Fuel Injection and Nozzle Cavitation

Valdas Caika and Peter Sampl
 AVL LIST GmbH

David Greif
 AVL Slovenia d.o.o.

ABSTRACT

To promote advanced combustion strategies complying with stringent emission regulations of CI engines, computational models have to accurately predict the injector inner flow and cavitation development in the nozzle. This paper describes a coupled 1D/2D/3D modeling technique for the simulation of fuel flow and nozzle cavitation in diesel injection systems.

The new technique comprises 1D fuel flow, 2D multi-body dynamics and 3D modeling of nozzle inner flow using a multi-fluid method. The 1D/2D model of the common rail injector is created with AVL software Boost-Hydsim. The computational mesh including the nozzle sac with spray holes is generated with AVL meshing tool Fame. 3D multi-phase calculations are performed with AVL software FIRE. The co-simulation procedure is controlled by Boost-Hydsim. Initially Hydsim performs a standalone 1D simulation until the needle lift reaches a prescribed tolerance (typically 2 to 5 μm). From this time instant the 1D/2D/3D co-simulation with the FIRE multiphase solver is started. During the co-simulation process Boost-Hydsim transmits to FIRE the displacement vector of the needle tip and fuel pressure and temperature at the nozzle interface. Based on this data, FIRE moves the computational mesh, adjusts boundary conditions, computes the time step and sends back to Boost-Hydsim the hydraulic force vector acting on the needle tip, sac pressure and mass flow rate through the needle seat and nozzle holes.

CITATION: Caika, V., Sampl, P., and Greif, D., "Integrated 1D/2D/3D Simulation of Fuel Injection and Nozzle Cavitation," *SAE Int. J. Engines* 6(3):2013, doi:10.4271/2013-24-0006.

INTRODUCTION

The basic 1D/3D nozzle flow simulation technique is already described in the previous works of the authors [1]. However, it was limited to 1D (longitudinal) needle motion both from 1D injector modeling in Boost-Hydsim and 3D nozzle flow calculation in FIRE. Moreover, only simple segment meshes with a single hole were considered. Now the co-simulation technique is extended in such a way that 2D motion of needle with 3 degrees-of-freedom can be simulated in Hydsim and corresponding mesh movement represented in FIRE. Using it the 1D and 2D (longitudinal and transverse) motion of the needle can be coupled with the 3D nozzle flow and cavitation model. In this way the new technique allows modeling of a non-uniform pressure distribution across the needle seat and nozzle holes.

Most of the cavitation models in fuel injection are based on the Eulerian or Lagrangian formulation or their combination [2]. Numerical and experimental investigation of cavitation in diesel nozzles has been carried out by Alajbegovic et al. [3], Arcoumanis et al. [4], Chen and Heister [5], Schmidt and Corradini [6], Sou and Kinugasa [7], Falcucci et al. [8] and other authors. A comprehensive survey of the cavitation models for diesel injection nozzles is provided by Giannadakis et al. [9]. Cavitating flow simulation in FIRE standalone using the standard multi-fluid method has been performed by Wang and Greif [10]. One-dimensional modeling of the injector needle and its effect on the nozzle cavitation has been studied by Čaika and Sampl [1] and Payri et al. [11].

THEORETICAL BASIS

Multi-Fluid Method in Nozzle Flow

Within the theory of the multi-phase flow, each phase is considered a continuum media and the conservation laws apply. An ensemble averaging is used to remove the microscopic interfaces. This results in macroscopic conservation equations analogous to their single-phase counterparts. The difference from single phase is the new variable (volume fraction) and new interfacial exchange terms. The averaged continuity and momentum equations can be derived from the work of Drew and Passman [12]:

$$\begin{aligned} \frac{\partial \alpha_k \rho_k}{\partial t} + \nabla \cdot \alpha_k \rho_k \mathbf{v}_k &= \Gamma_k, \\ \frac{\partial \alpha_k \rho_k \mathbf{v}_k}{\partial t} + \nabla \cdot \alpha_k \rho_k \mathbf{v}_k \mathbf{v}_k &= \\ -\alpha_k \nabla p + \nabla \cdot \alpha_k \tau_k + \alpha_k \rho_k \mathbf{g} + \mathbf{M}_k + \mathbf{v}_{\text{int}} \Gamma_k, \end{aligned} \quad (1)$$

where α , ρ , \mathbf{v} and p are the averaged volume fraction, density, velocity and pressure, respectively, the subscript k denotes a phase indicator, \mathbf{v}_{int} is the interfacial velocity, Γ_k is the phase change rate and \mathbf{M}_k is the interfacial momentum transfer term. Essential term in the cavitation modeling is the vaporization rate, or the interfacial mass exchange Γ_k . In our cavitation model it is governed by the Rayleigh equation for the single bubble dynamics:

$$r\ddot{r} + \frac{3}{2}\dot{r}^2 = \frac{\Delta p}{\rho_l}, \quad (2)$$

where r is the bubble radius and Δp is the effective pressure difference. The mass change rate of a single bubble is:

$$\Gamma = 4\pi r^2 \rho_b \dot{r}. \quad (3)$$

For a population of bubbles with a distribution function f , defined as the number of bubbles within the radius span of $(r, r+dr)$, the total mass transfer rate is given by:

$$\Gamma_v = \int_0^\infty f(r) 4\pi r^2 \rho_b \dot{r} dr. \quad (4)$$

More details on the multi-phase flow application and bubble cavitation in injection nozzles can be found in [13].

Modeling of Injector Flow and Motion of Mechanical Parts

Model of the injector flow (except nozzle) in Boost-Hydsim is based on the one-dimensional theory of weakly-compressible fluid mechanics [14]. Pressure wave propagation in lines is calculated using variable fluid density and velocity of sound. Two-dimensional needle motion with

3 degrees-of-freedom (translation along x, y and z axes) and one-dimensional motion of other mechanical components (control valve body, pistons of hydraulic amplifier) is calculated by the classical theory of multi-body dynamics. Axial needle deformation due to varying pressure is considered by linear elasticity. For the leakage modeling in the clearance of the needle guide laminar flow theory is applied. Electric charge, mechanical strain and deformation of the piezoelectric stack actuator are obtained from the electro-mechanical lumped-parameter model:

$$\begin{aligned} q &= n \cdot x_n + C_n \cdot V_t, \\ V_t &= V_{\text{in}} - V_{\text{rc}}, \\ V_{\text{rc}} &= mrc(q), \\ F_t &= n \cdot V_t, \\ m_n \cdot \ddot{x}_n + b_n \cdot \dot{x}_n + k_n \cdot x_n &= F_t + F_{\text{ext}}, \end{aligned} \quad (5)$$

where q is the charge of the piezoelectric stack, n is the electromechanical transformer ratio, x_n is the endpoint displacement of the stack, C_n is the stack electrical capacitance, V_{in} is the input voltage applied on the stack, V_{rc} is the voltage loss due to hysteresis, V_t is the back electromotive force from the mechanical domain, F_t is the transduced force from the electrical domain, m_n , b_n and k_n are the mass, damping and stiffness of the piezoelectric stack, respectively, N_L is the number of ceramic layers, F_{ext} is the force imposed from the external load and $mrc()$ is the function relating the voltage across the resistive capacitor element to the charge in the ceramic layer. Further details on the modeling of the piezoelectric stack can be found in [15].

INJECTOR MODEL

Injector in question is a piezo-controlled common rail injector CRI3 from Bosch [16]. Basic features of the CRI3 injector are sharp injector rate, small pilot injection quantity (0.5 mm^3), reduced tolerances for low emission standards, multiple injections (up to 7 per cycle), reduced static and dynamic forces, fail-safe-principle, low noise and compact design. The injector is designed for the rail pressure up to 180 MPa (CRI3.1) and 200 MPa (CRI3.2), respectively. Schematic of the injector is shown in Figure 1. The main components of the injector are piezoelectric stack actuator, hydraulic amplifier (coupler), control valve, throttle plate and nozzle. Nozzle design is shown in Figure 2. Hydsim models of the lower and upper injector parts are shown in Figure 3 and Figure 4.

The piezoelectric stack actuator consists of a dense pile of separately contacted layers (wafers) of electrically active ceramic material. The layers are assembled mechanically in series and connected electrically in parallel. With voltage applied, electric field across the ceramic layers induces a mechanical strain, which results in the stack elongation. Detailed description of the stack actuator is given in [15].

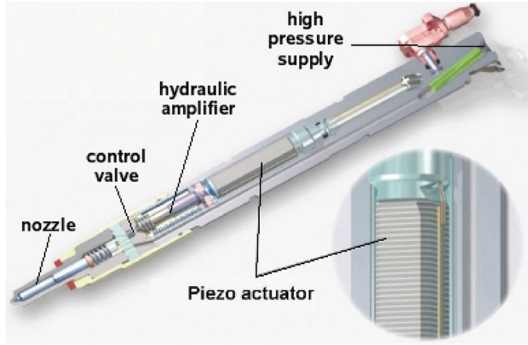


Figure 1. Schematic of CRI3 piezoelectric injector.

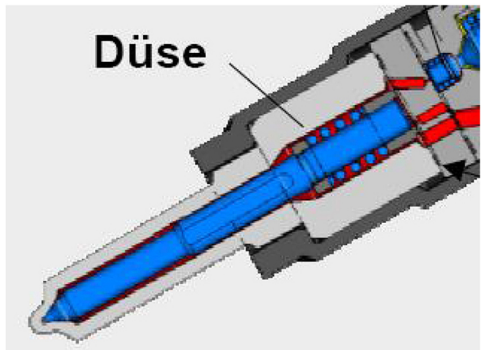


Figure 2. Nozzle with needle and throttle plate.

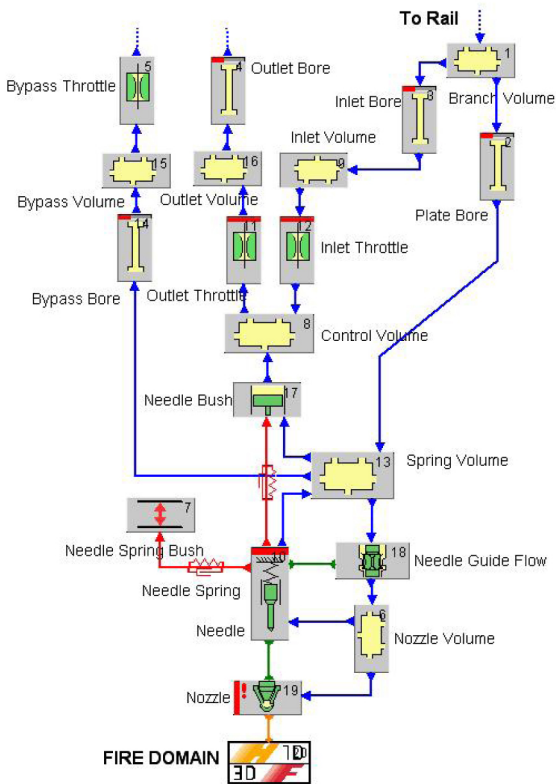


Figure 3. Boost-Hydsim model of injector nozzle.

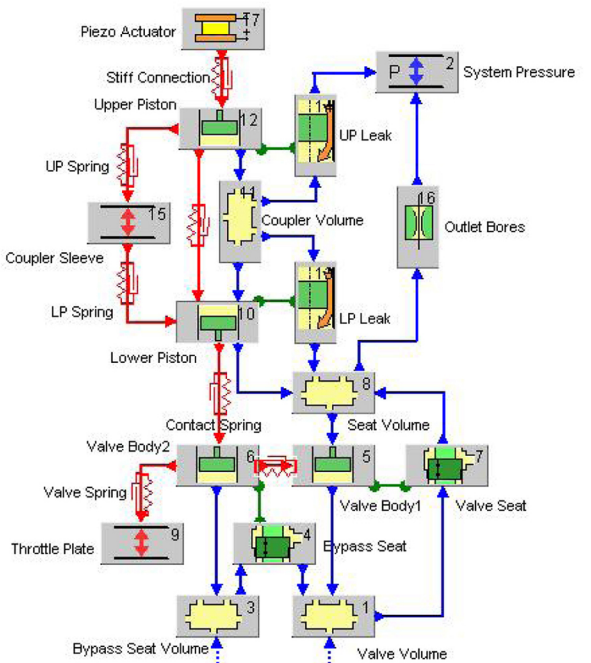


Figure 4. Boost-Hydsim model of piezoelectric actuator and hydraulic amplifier.

COUPLING INTERFACE

Hydsim-FIRE coupling interface is illustrated in Figure 5. The red dashed line along the needle tip contour separates the 1D simulation domain (Hydsim) from the 3D domain (FIRE). Figure 5 shows the centered 1 DOF needle case (with one degree-of-freedom and one force component). Extended interface with eccentric 3 DOF needle (3 degrees-of-freedom and 3 force components) is shown in Figure 6. Forces acting on the 3DOF needle are depicted in Figure 7. Parameter h_{interf} denotes the interface height, i.e. the distance from the needle seat to the border line between 1D and 3D domains.

On each exchange step FIRE transfers to Boost-Hydsim the following data:

- \mathbf{F}_N - force vector acting on needle tip
- q_{seat} - flow rate through needle seat
- q_{holes} - flow rate through nozzle holes
- p_{topV} - boundary pressure below interface line
- T_{topV} - boundary temperature below interface line
- p_{sac} - average pressure in sac volume
- T_{sac} - average temperature in sac volume
- p_{gas} - boundary pressure in spray chamber
- T_{gas} - boundary temperature in spray chamber

At the end of the exchange time step Boost-Hydsim transfers to FIRE the following data:

- X_d - displacement vector of needle tip
- p_{nozV} - boundary pressure above interface line
- T_{nozV} - boundary temperature above interface line

Our injector example considers both cases: centered needle model with 1 degree-of-freedom (longitudinal motion in z) and eccentric needle with 3 degrees-of-freedom (linear motion in x, y and z). The needle lift tolerance in axial direction (z) for co-simulation start is set to 2 μm . Axial needle motion is calculated from the injector dynamics. To initiate radial needle motion in 3 DOF case, the initial condition along x axis is set to $-1 \mu\text{m}$ (along y axis it is 0). With this starting condition, as long as the needle tip interferes with the conical seat contour, kinematic needle movement along the seat surface is imposed. Dynamic calculation of x and y motion starts when axial lift is high enough so that the needle tip gets out of contact with the seat. Note that needle motion in radial direction is limited by the cylindrical gap between needle guide and nozzle body. In light duty common rail injectors this diametric gap is typically 4 to 5 μm . In our model we allow the gap up to 9 μm . If radial needle motion overcomes this gap, the injector wall reaction force is calculated and applied on the needle guide. In the actual implementation this calculation is performed in a simplified way by introducing a stiff linear spring and damper at the contact (without consideration of the fluid film effects). Hydsim calculation step is 10^{-7} s , exchange step with FIRE is 10^{-6} s . This step is effective only for the intervals where axial needle lift exceeds the tolerance (i.e. during injection).

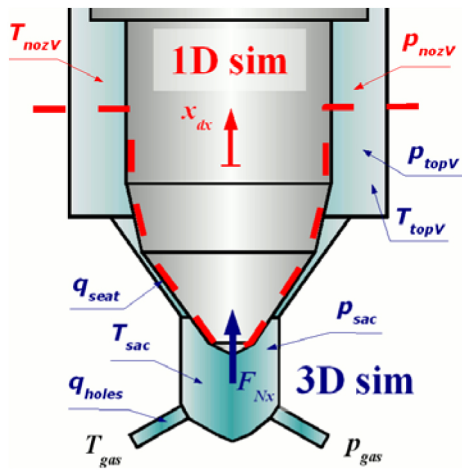


Figure 5. Coupling interface with exchange variables.

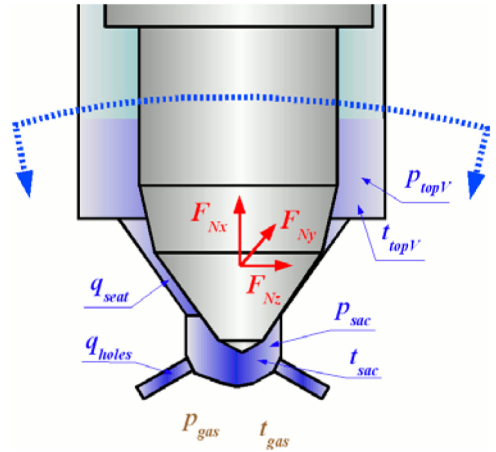


Figure 6. Calculation domain with eccentric needle.

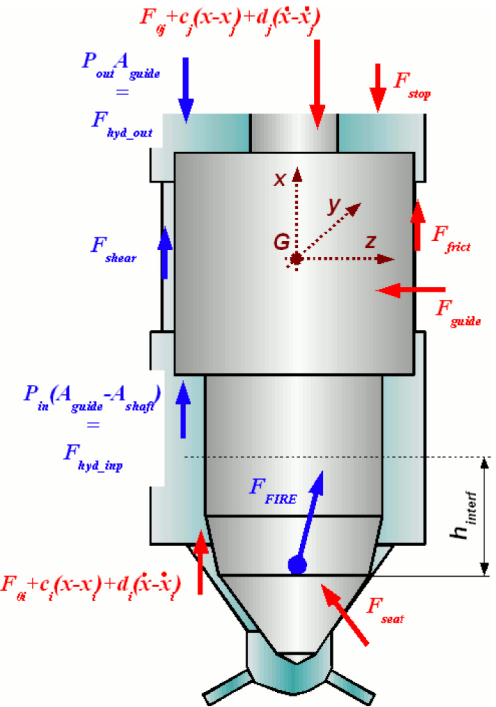


Figure 7. Forces acting on 3 DOF needle (red - mechanical, blue - hydraulic).

NOZZLE MESH

Computational grid used in the CFD simulation is shown in Figure 8, Figure 9 and Figure 10 (different views). The mesh consists of the hollow cylinder around the needle shaft, needle seat area with nozzle sac and eight cylindrical holes. For the case with 1 DOF needle, only one of the eight periodic 45-degree-segments is modeled (refer to [1]). For the new case with 3 DOF needle, the full 360-degree symmetric mesh is created. It consists of 845280 hexahedral cells with 240 cell layers in the circumferential direction, so that one layer corresponds to 1.5 degrees. Cell size in the narrowest

needle seat gap is $0.3 \times 25 \mu\text{m}$. The outlet bores are meshed separately and connected to the sac volume by arbitrary-interfaces. The nozzle gap itself contains 50 cell rows in the radial direction and 11 rows in vertical direction. The mesh topology is chosen according to AVL experience with nozzle flow simulation [13]. Needle movement is accomplished by the mesh-deformation at solver run-time. The mesh-deformation-function shifts the needle surface at each time step according to the needle displacement vector received from Hydsim. After that, the position of the internal nodes is updated by the Laplace interpolation scheme. To prevent collapsing of cells at zero or very small needle lift, a minimal gap size is maintained in the mesh ($3 \mu\text{m}$ in the actual case).

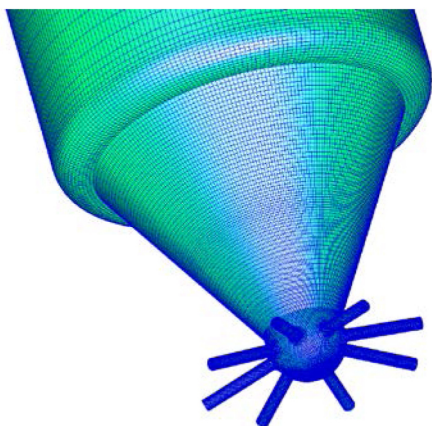


Figure 8. Computational grid (general view).

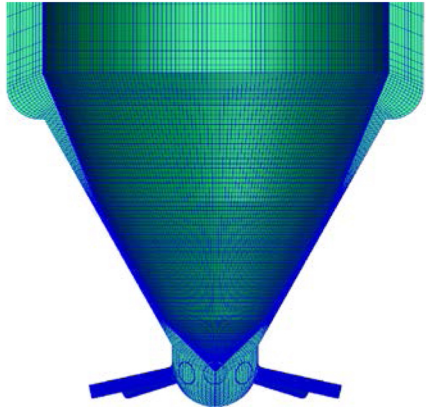


Figure 9. Nozzle mesh: cross-section with needle tip.

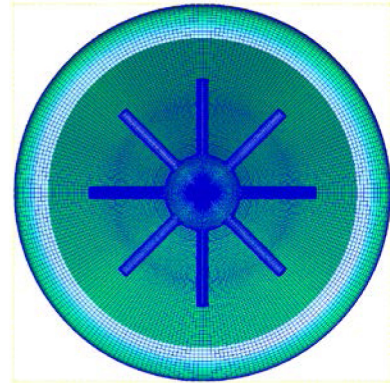


Figure 10. Nozzle mesh: bottom view.

CALCULATION RESULTS

Calculation is carried out for one load case corresponding to the engine speed 2000 rpm and rail pressure 160 MPa. As our primary interest lies in the investigation of nozzle flow and cavitation at small needle lifts, only a pilot injection is analyzed. This also allows keeping the computational effort within a reasonable range. Two needle models with 1 DOF and 3 DOF are considered. Selected calculation results from Boost-Hydsim postprocessor are shown in [Figure 11](#) (needle and actuator motion) and [Figure 12](#) (pressure and flow rate). For convenience they are plotted in the crank angle domain. Maximum needle lift is about $50 \mu\text{m}$ and injection quantity is 2.2 mm^3 . Actuation voltage is applied to piezoelectric actuator at 3.2 deg crank angle. Needle opens (injection begins) at 5.6 deg crank angle. Hence time delay between the actuation start and injection start is 2.4 deg or $200 \mu\text{s}$. Note that at 5.6 deg crank angle the co-simulation between Boost-Hydsim and FIRE begins. Comparing needle motion and injection rate for 1 DOF and 3 DOF cases, one can observe that axial needle lift and injection rate are nearly same for both needle models. As the nozzle mesh is fully symmetric, radial needle motion in our model is excited by the initial displacement of $-1 \mu\text{m}$ along x axis (along y axis the initial condition is 0). Due to this the radial needle movement occurs only along x axis. As shown in [Figure 11](#) (bottom graph), after opening the needle moves along x axis from the initial shift towards the center position, crosses the symmetry axis and finally reaches $4.5 \mu\text{m}$ position on the opposite side. Till the contact with the nozzle wall needle motion is determined by the radial force from CFD simulation. During contact needle gets bounced back by the guide reaction forces (calculated by Hydsim) and returns towards the center position. Note that pressure in servo valve volume (element 1 in [Figure 4](#)) drops from 160 to 15 MPa.

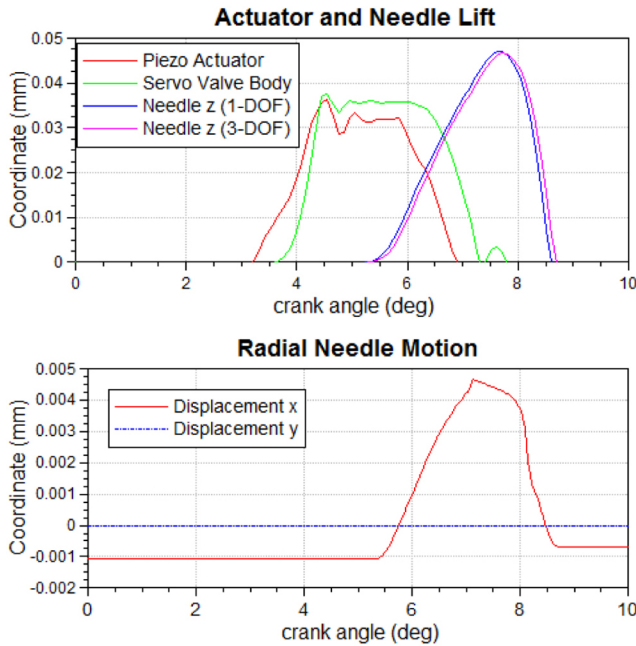


Figure 11. Stack Actuator and needle motion for 1 DOF and 3 DOF needle cases.

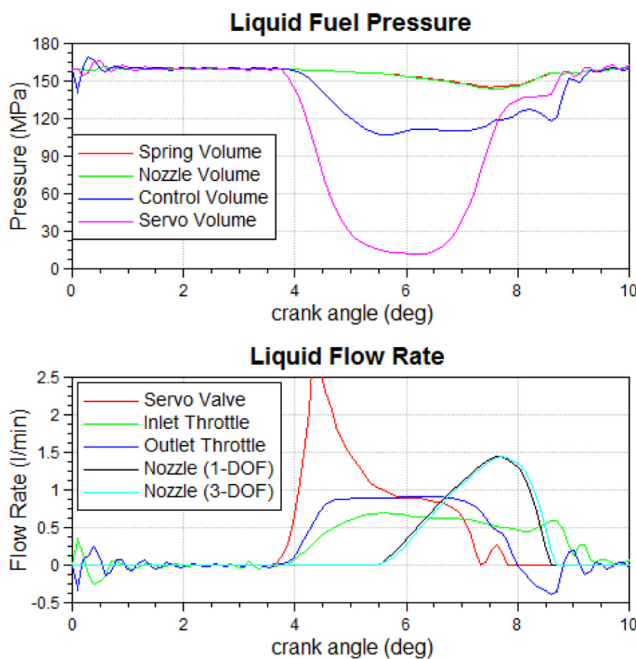


Figure 12. Fuel pressure and flow rate in injector for 1 DOF and 3 DOF needle cases.

Characteristic 3D calculation results are volume fraction, liquid pressure and velocity. Volume fraction for 3 DOF case is shown in [Figure 13](#) (at two opening instants) and [Figure 14](#) (at two closing instants). There blue color represents 100% diesel liquid, red color - 100% diesel vapor. Note that needle reaches the prescribed tolerance of 2 μm at Hydsim crank angle 5.6 deg (this corresponds to zero time in FIRE).

On the very opening, at needle lift of 3 μm (FIRE time 5 μs) light vaporization area is visible above the open side of the needle seat (due to eccentricity) which slowly vanishes within the next steps. From 10 μm lift till full lift of 47 μm cavitation does occur neither at seat nor in the holes. The needle seat starts cavitating again when the lift drops to 40 μm (FIRE time 190 μs). From the lift of about 20 μm (FIRE time 235 μs) till needle closing (FIRE time 250 μs) cavitation ring at needle seat contracts gradually to the wider open area (due to radial shift) and spreads into the sac and holes. Note that different holes exhibit different cavitation patterns. In several holes cavitation area propagates till the outlet.

[Figure 15](#) shows the pressure distribution in the nozzle. At opening one can clearly distinguish between the rail pressure (160 MPa) above the needle seat and outlet pressure (2 MPa) behind it. With the higher needle lift, the pressure in the nozzle sac gradually increases, and one can observe a continuous pressure drop across the seat. Due to the radial needle shift, the pressure distribution in the circumferential direction is not uniform, i.e. pressure around the seat stays higher at the narrower gap, thus inducing a radial force which is transferred to Hydsim and pushes the needle towards the central position. This effect can be observed not only at seat but also at needle guide if the latter gets close to the nozzle wall. Generally, at higher needle lifts, the radial needle motion is mainly limited by the gap width between the guide and nozzle wall. As stated earlier, the guide reaction force at its contact with the wall is calculated directly by Hydsim using a simplified method.

[Figure 16](#) depicts the liquid velocity in the nozzle. Naturally, higher velocities occur in the wider open seat area, where needle eccentricity is the largest. Due to this effect the liquid velocities may get higher in the holes which are located closer to the wider open seat area. However, this strongly depends on the flow conditions in the nozzle sac. The highest velocity of about 400 m/s occurs at maximum needle lift of 47 μm at 7.6 deg (FIRE time 130 μs).

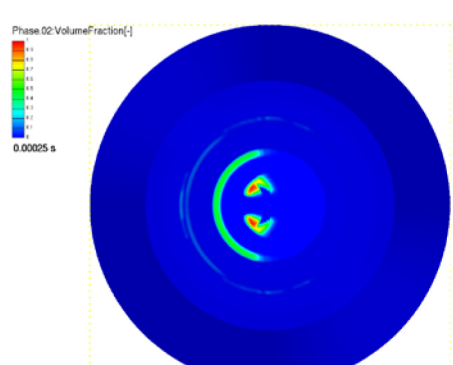
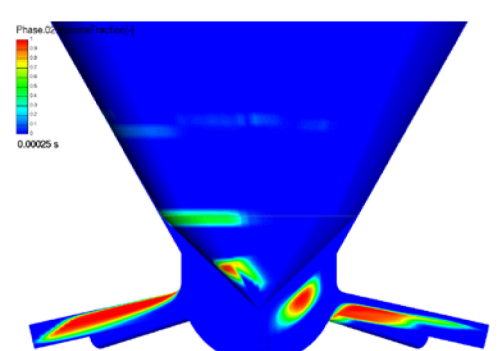
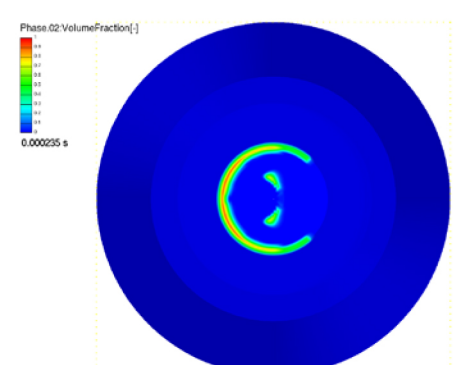
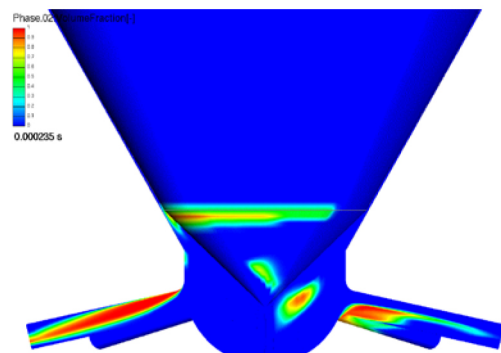
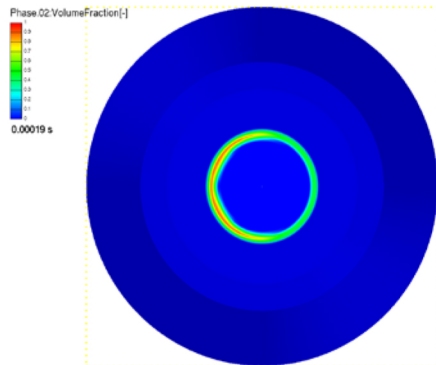
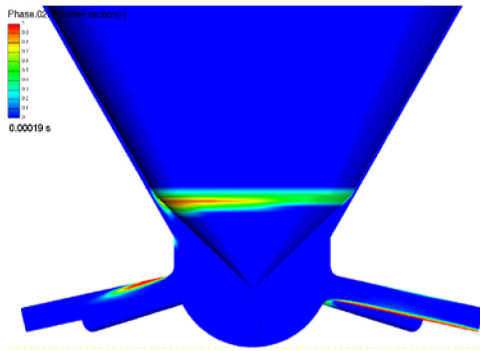
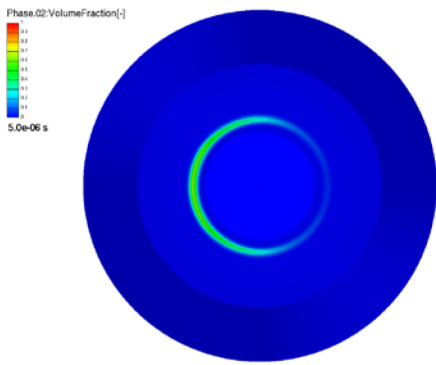
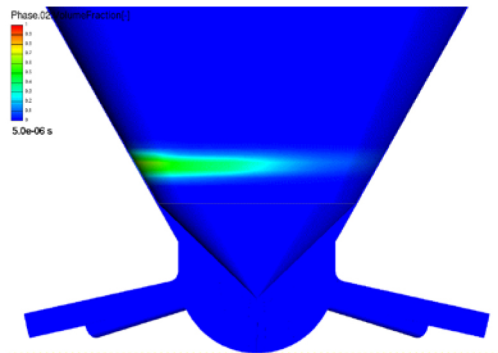


Figure 13. Volume fraction for 3 DOF needle at opening (time instants 5 μ s and 190 μ s); 1st and 3rd images - mid plane cut, 2nd and 4th images - bottom view on needle tip)

Figure 14. Volume fraction for 3 DOF needle at closing (time instants 235 μ s and 250 μ s); 1st and 3rd images - mid plane cut, 2nd and 4th images - bottom view on needle tip)

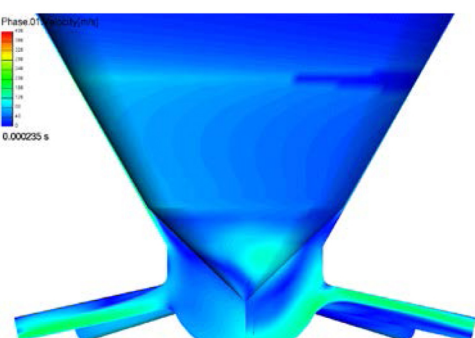
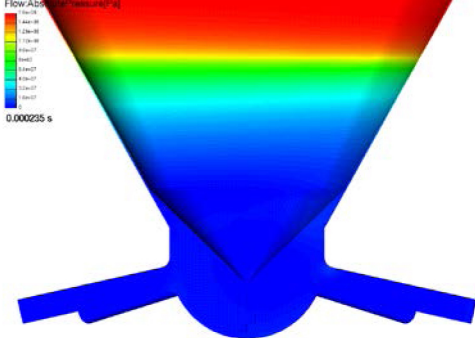
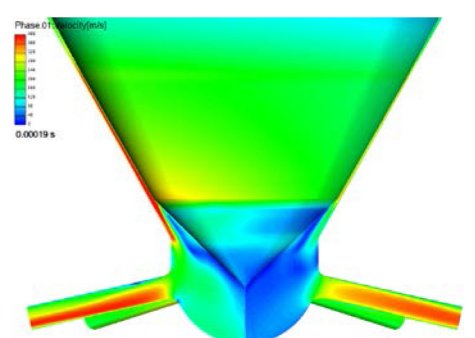
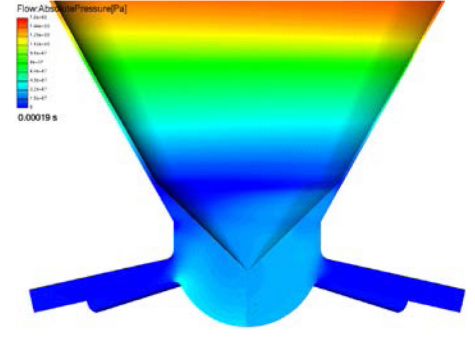
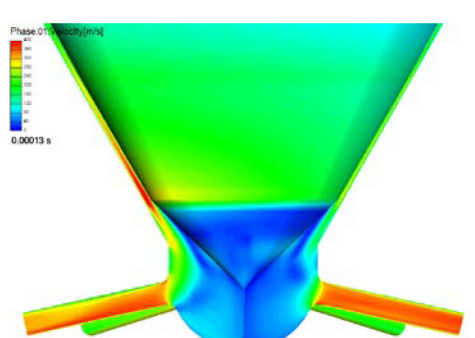
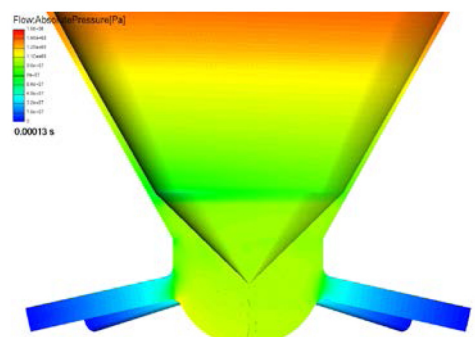
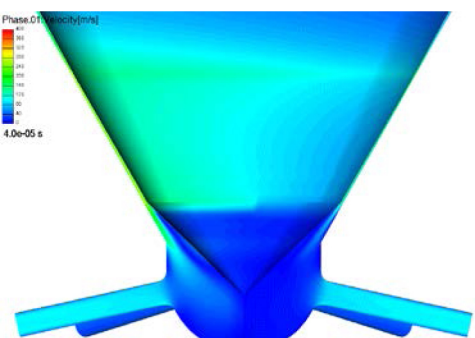
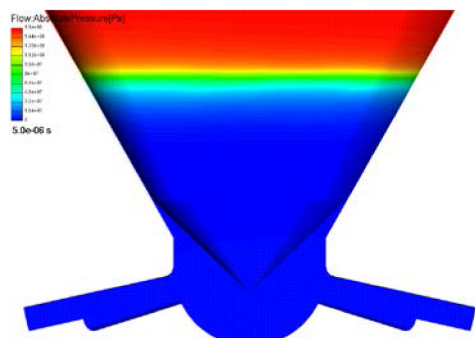


Figure 15. Liquid phase pressure at time instants (from top): 5 μ s, 130 μ s (opening), 190 μ s and 235 μ s (closing)

Figure 16. Liquid phase velocity at time instants (from top): 5 μ s, 130 μ s (opening), 190 μ s and 235 μ s (closing)

CONCLUSION

Novel 1D/2D/3D flow simulation technique for fuel injection and nozzle cavitation analysis is developed. It is based on the 3D multi-fluid method in the commercial CFD code AVL FIRE and 1D fluid flow and 2D multi-body dynamics in AVL Boost-Hydsim software. Basically, the new technique is a substantial extension of 1D/3D nozzle flow simulation method earlier published by the authors. The previous technique was limited to 1D (longitudinal) needle motion both from 1D injector modeling in Boost-Hydsim and 3D nozzle flow calculation in FIRE. Now both software tools are extended in such a way that 2D motion of the needle with 3 DOF (translation in x, y and z) can be simulated in Boost-Hydsim and respective mesh movement represented in FIRE. Using this technique, a 1D/2D (longitudinal and transverse) motion of the needle can be coupled with the 3D nozzle flow and cavitation model as shown in the demonstration example. This allows modeling of a non-uniform pressure distribution and cavitating flow across the needle seat and nozzle holes.

REFERENCES

1. Caika, V. and Sampl, P., "Nozzle Flow and Cavitation Modeling with Coupled 1D-3D AVL Software Tools," SAE Technical Paper [2011-24-0006](#), 2011, doi:[10.4271/2011-24-0006](#).
2. Edelbauer, W., "Coupling of 3D Eulerian and Lagrangian Spray Approaches in Industrial Combustion Engine Simulation," ILASS, 24th European Conf. on Liquid Atomization and Spray Systems, Portugal, 2011, 108-119.
3. Alajbegovic, A., Grogger, H. and Phillip, H., "Calculation of Transient Cavitation in Nozzle using Two-Fluid Method," Int. Conf. on Liquid Atomization and Spray Systems, Indianapolis, IN, USA, 1999, 209-213.
4. Arcoumanis, C., Flora, H., Gavaises, M., and Badami, M., "Cavitation in Real-Size Multi-Hole Diesel Injector Nozzles," SAE Technical Paper [2000-01-1249](#), 2000, doi:[10.4271/2000-01-1249](#).
5. Chen, J. and Heister, D., "Modeling Cavitating Flows in Diesel Injectors," *Atomization and Sprays*, 6, 709-726, 1996.
6. Schmidt, D. and Corradini, M., "The Internal Flow of Diesel Fuel injector Nozzles," *Int. J. Engine Research*, 2, 1-22, 2001.
7. Sou, A. and Kinugasa, T., "Numerical Simulation of Developing Cavitating Flow in a Nozzle of Pressure Atomizer," THIESEL Conf. on Thermo- and Fluid Dynamic Processes in Engines, Valencia, Spain, 2010.
8. Falcucci, G., ubertini, S., Bella, G., Palpacelli, S. et al., "Lattice Boltzmann Simulation of a Cavitating Diesel Injector Nozzle," SAE Technical Paper [2011-24-0008](#), 2011, doi:[10.4271/2011-24-0008](#).
9. Giannadakis, E., Gavaises, M. and Arcoumanis, C., "Modeling of Cavitation in Diesel Injector Nozzles," *J. Fluid Mechanics*, 616, 153-193, 2008.
10. Wang, D. and Greif, D., "Progress in Modeling Injector Cavitating Flows with a Multi-fluid Method," ASME Forum on Cavitation and Multiphase Flow, Miami, FL, USA, 2006.
11. Payri, F., Margot, X., Patouna, S., Ravet, F. et al., "A CFD Study of the Effect of the Needle Movement on the Cavitation Pattern of Diesel Injectors," SAE Technical Paper [2009-24-0025](#), 2009, doi:[10.4271/2009-24-0025](#).
12. Drew, A. D., and Passman, S. L., "Theory of Multicomponent Fluids," New York: Springer, 1999.
13. Greif, D. and Srinivasan, V., "Numerical Prediction of Erosive Cavitating Flows in Injection Equipment," SAE Technical Paper [2011-24-0004](#), 2011, doi:[10.4271/2011-24-0004](#).
14. AVL Boost-Hydsim, User's Guide, Graz, 2013.
15. Caika, V., Kammerdiener, T., and Dörr, N., "Operation of Piezoelectric Common Rail Injector with Diesel and FT-Kerosene," SAE Technical Paper [2007-24-0070](#), 2007, doi:[10.4271/2007-24-0070](#).
16. Boecking, F. et al., "Passenger Car Common Rail Systems for Future Emission Standards," *MTZ* 7-8, 66, 552-557, 2005.

CONTACT INFORMATION

Dr. Valdas Čaika
AVL LIST GmbH
Hans-List-Platz 1, A-8020 Graz, Austria
valdas.caika@avl.com